CZASOPISMO INŻYNIERII LĄDOWEJ, ŚRODOWISKA I ARCHITEKTURY
JOURNAL OF CIVIL ENGINEERING, ENVIRONMENT AND ARCHITECTURE
JCEEA, t. XXXV, z. 65 (4/18), październik-grudzień 2018, s. 103-112, DOI:10.7862/rb.2018.60

Roman VODIČKA[1]
Katarína KRAJNÍKOVÁ[2]
Lucia BARANOVÁ[3]

APPLICATION OF AN INTERFACE DAMAGE MODEL TO STEEL REINFORCED CONCRETE: A STUDY OF THE SIZE EFFECT

Influence of the size of steel reinforcement of a concrete structure on crack initiation at the interface between the steel fibre and the concrete body of the structure is under consideration. Numerical analysis is provided using a quasi-static delamination model for interface rupture based on an energetic approach using a cohesive zone model for providing the interface stress-strain relation. The obtained results confirm expected dependence of the critical load which causes triggering of the interface crack on a structure dimension parameter.

Keywords: interface crack, damage evolution, quasi-static delamination, critical load, crack mode

1. Introduction

Several experiments confirmed that the size of a fibre placed in a fixed volumetric unit of a composite material influences various macroscopic properties of such composites. For instance, the tensile strength was found to depend on the size of an inclusion in works of Fisher et al. [3] or Cho et al.[2]. Such a kind of the size effect was explained by using different cohesive zone models (CZM) for describing the interface stress-strain relations by Carpinteri et al. [1], or Tavara et al. [9]. Based on such results, the aim of the present work is to apply the model developed in [5][10] to a problem which leads to the

[1] Corresponding author: Roman Vodička, Faculty of Civil Engineering, Institute of Construction Technology and Management, Technical University of Košice, Vysokoškolská 4, 042 00 Košice, Slovakia, +421 602 4388, roman.vodicka@tuke.sk

[2] Katarína Krajníková, Faculty of Civil Engineering, Institute of Construction Technology and Management, Technical University of Košice, Vysokoškolská 4, 042 00 Košice, Slovakia, +421 602 4386, lucia.baranova@tuke.sk

[3] Lucia Baranová, Faculty of Civil Engineering, Institute of Construction Technology and Management, Technical University of Košice, Vysokoškolská 4, 042 00 Košice, Slovakia, +421 602 4386, katarina.krajnikova@tuke.sk

aforementioned size effect. Additionally, numerical tests also show the dependence of the size effect on the transverse loading, as shown by Carpinteri et al. [1], or Mantič [6][7], therefore the proposed tests are to demonstrate in some sense such influences by introducing various boundary conditions in the solved problem.

The predictions of interface failure are calculated by implementing a quasi-static rate-independent model of interface rupture which uses a bilinear CZM as in [11]. The evolution in time is governed by the total potential energy functional E and the functional of energy dissipation R [8][12].

The evolution model is described in Section **Błąd! Nie można odnaleźć źródła odwołania.**, very briefly with underlying energy functionals. The main part of the analysis is summarizes in Section **Błąd! Nie można odnaleźć źródła odwołania.**, where the size effect is assessed in a particular example of steel fibre reinforcement placed in concrete matrix.

2. A brief description of the interface damage model

The section briefly reviews the mathematical formulation of the used model which is based on energy balance. The total potential energy E is given by the mechanical energy stored in the bulk and at the interface as a function of displacements u and the internal variable for interface damage ζ, ($0 \le \zeta \le 1$), decreasing from 1 (undamaged state) to 0 (crack initiation and propagation), i.e. $\dot{\zeta} \le 0$. The damage evolution is considered rate independent so that the dissipation potential R, being a degree one positively homogeneous function of the damage rate $\dot{\zeta}$, is also the dissipation rate. The model consists of linear elastic solids in contact along adhesive interfaces whose constitutive law includes both a linear elastic and a softening branch. The numerical approach is formulated as a recursive time-stepping procedure for finding local minima of the sum of the changes of total potential and dissipated energies, one with respect to u and the other with respect to ζ. By a special choice of the interface energy functional, the interface constitutive relation of the bilinear CZM is obtained in the following form, cf. [11]:

$$p_{\mathrm{n}} = k_{\mathrm{n}}\phi(\zeta)\delta_{\mathrm{n}} + k_{\mathrm{g}}\langle\delta_{\mathrm{n}}\rangle_{-}, \quad p_{\mathrm{t}} = k_{\mathrm{t}}\phi(\zeta)\delta_{\mathrm{t}}, \quad \phi(\zeta) = \tfrac{\beta\zeta}{1+\beta-\zeta}, \beta > 0 \text{ on } \Gamma_{\mathrm{c}} \qquad (1)$$

where $p_{\mathrm{n}}(x)$ and $p_{\mathrm{t}}(x)$, respectively, are the normal and tangential components of the interface tractions, $\delta_{\mathrm{n}}(x)$ and $\delta_{\mathrm{t}}(x)$, respectively, are the normal and tangential relative displacements between opposite interface points, i.e. $\delta = u^{\mathrm{A}} - u^{\mathrm{B}}$ (superscripts A and B refer to the bodies adjacent to the interface from both its sides), k_{n} and k_{t}, respectively, denote the normal and tangential stiffnesses of the adhesive in the interface. The additional term with $\langle\delta_{\mathrm{n}}\rangle_{-}$, denoting the negative

part of the relative normal displacement, provides the normal compliance contact model with finite interpenetration ($k_g >> k_n$) at the interface Γ_c.

The interface damage (and subsequent crack) evolution is controlled by the energy release rate G whose critical value $G_d(\delta)$ is the fracture energy being defined as fracture-mode sensitive, e.g. according to the Hutchinson-Suo law [4]

$$G_d(\delta) = G_{Id}\left(1 + \tan^2\left(\left(\frac{2}{\pi}\arctan\sqrt{\frac{G_{IId}-G_{Id}}{G_{Id}}}\right)\arctan\left|\sqrt{\frac{k_t}{k_n}}\frac{\delta_t}{\langle\delta_n\rangle_+}\right|\right)\right), \tag{2}$$

where the parameters G_{Id} and G_{IId} express the fracture energies in the pure Mode I and in the pure Mode II, respectively, and $\langle\delta_n\rangle_+$ denotes the positive part of the relative normal displacement to exclude a state of compression from damage propagation.

2.2. Energetic formulation of the model

Let us consider the energies which are taken into account in the model for two domains Ω^A and Ω^B with boundaries Γ^A and Γ^B, respectively. The stored energy functional is defined as

$$\begin{aligned} E(\tau;u,\zeta) = &\int_{\Gamma^A}\frac{1}{2}u^A.p^A(u)\,d\Gamma + \int_{\Gamma^B}\frac{1}{2}u^B.p^B(u)\,d\Gamma + \\ &\int_{\Gamma_c}\frac{1}{2}\left[k_n\phi(\zeta)\delta_n^2 + k_t\phi(\zeta)\delta_t^2 + k_g\langle\delta_n\rangle_-^2\right]d\Gamma, \end{aligned} \tag{3}$$

for the admissible (time τ dependent) displacement $u^\eta = w^\eta(\tau)$ on a part of boundary Γ_u^η with η=A, or B. The first two integrals, representing the elastic strain energy in the subdomains Ω^η, are expressed in their boundary form. The last integral is the interface term which corresponds to the expected interface stress-strain relation (1).

The potential energy of external forces (acting only along a part of the boundary denoted Γ_p^η) is given by the relation

$$F(\tau;u) = -\int_{\Gamma_p^A} f^A.u^A\,d\Gamma - \int_{\Gamma_p^B} f^B.u^B\,d\Gamma, \tag{4}$$

where $f^\eta(\tau)$ are the prescribed forces on the part of boundary Γ_p^η . The dissipated energy is introduced by the (pseudo)potential R which reflects the rate-independence of the debonding process

$$R\left(u;\dot{\zeta}\right)=\int_{\Gamma_c} G_d(\delta)\left|\dot{\zeta}\right| \mathrm{d}\Gamma, \tag{5}$$

with fracture energy defined by (2). The relations which govern the evolution of damage can be written in form of nonlinear variational inclusions with initial conditions

$$\begin{aligned} &\partial_u E(\tau; u, \zeta) + \partial_u F(\tau; u) \ni 0, \qquad u(\tau=0)=u_0, \\ &\partial_{\dot{\zeta}} R\left(u;\dot{\zeta}\right) + \partial_{\zeta} E(\tau; u, \zeta) \ni 0, \quad \zeta(\tau=0)=\zeta_0, \end{aligned} \tag{6}$$

where ∂ denotes (partial) subdifferential of a convex non-smooth function, see [8], which can be replaced by Gateaux differential if the functional is sufficiently smooth, as e.g. F. The initial condition for damage is usually ζ_0=1, pertaining to the undamaged state. It should also be noted that the energy release rate G is hidden in the second inclusion of (6) as it expresses a change of energy E due to a change of damage ζ.

3. Prediction of the size effect for a steel inclusion

The size effect for a steel-concrete structure may be caused by changing size of the steel inclusion. It can be modelled as a variable-size inclusion in a fixed matrix size representing a volumetric unit of the whole structure. Of course, also other dimension changes can be applied. The size effect also depends on the type and the form of the loading. Therefore, several types of boundary constraints will be taken into account.

In the described model, the damage initiation pertains to the instant when ζ<1 and crack initiation to the instant when ζ=0. The difference between these two instants determines the cohesive zone in the interface. In order to eliminate influence of the cohesive zone in the numerical analysis, the two instants are set actually close to each other by appropriate adjusting of the model parameter.

3.1. Problem definition

The geometry of the solved problem is shown in Fig. 1, where three choices of the applied boundary conditions are depicted, all of them using the dimensions a and r. In all cases, compression is considered. It can be guessed that no significant difference appears between the cases (A) and (B). The case (C), however, corresponds to a biaxial load, in fact compression, therefore the form of the size effect may be distinct. The changes of critical loads depending on the actual scale of the domain will be done in three modes:

I. Inclusion changing size.
II. Matrix changing size.
III. Inclusion and matrix changing sizes proportionally.

The material parameters of the domains are E=210 GPa, ν=0.3 for the steel inclusion, and E=20 GPa, ν=0.2 for the concrete matrix. The interface characteristics

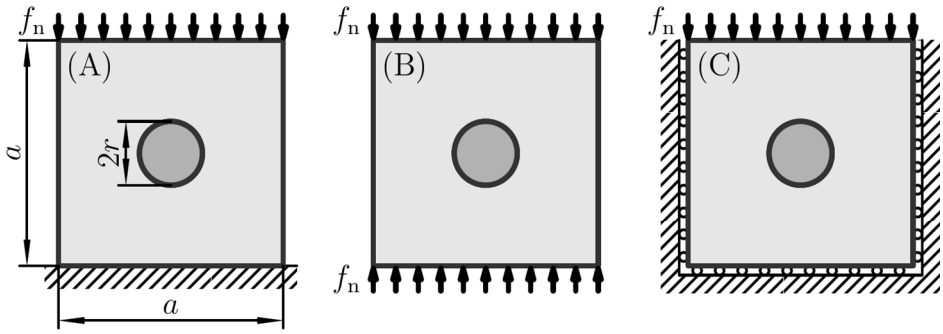

Fig. 1. Geometry of the solved problem and three options of boundary conditions

for the physical model are based on the assumptions that maximal normal tensile stress is p_n^c =25 MPa, and fracture energy for an opening crack is G_{Id}=0.101 kJm^{-2}, the bilinear CZM (1) is considered such that it provides an almost brittle interface, which occurs, if the parameter β is large, namely β=100. The model is crack mode sensitive if G_{IId} is different from G_{Id}, namely G_{IId}=0.690 kJm^{-2}, so that for the choice of the interface stiffnesses in (1) or (2) k_n=3.125 TPam^{-1}, and $k_t = 0.25k_n$ the maximal shearing stress is p_t^c =32.66 MPa.

The loading f in (4) prescribed by the normal pressure f_n is applied in increments until total rupture occurs at a part of the interface. The main aim is to find the critical value of the load f_n^c at which the interface crack is initiated. The discretisation has the time step τ=0.01 s which causes also the load step 0.01 MPa. The interface is discretised by 128 boundary elements.

3.2. Results

We intend to compare the critical magnitudes of the applied load f_n^c as functions of some characteristic dimension of the structure for the three introduced in Fig. 1 configurations. Simultaneously we try to explain changes in graph curves based on some observations for stresses. Generally, the boundary conditions (C) cause biaxial compression so that normal stresses cannot initialize damage and the crack appears in Mode II. An effect of the boundary conditions (A) and (B) is similar, therefore also the results in these two cases are similar for each of the scaling options I, II, and III. Additionally, the crack mode can be separated due to the fact that at the places with the maximal normal tensile stress the tangential stress vanish or it is close to zero, and at the places with the maximal absolute value of the tangential stress the normal stress

is compressive not affecting the damage evolution and a crack propagation. Therefore, if the ratio $\left|p_{\mathrm{t}\max}\right|/\left(\left\langle p_{\mathrm{n}}\right\rangle_{+}\right)_{\max}$ is greater than $p_{\mathrm{t}}^{\mathrm{c}}/p_{\mathrm{n}}^{\mathrm{c}}=1.31$, a crack appears in Mode II, otherwise it is in Mode I.

The first size changing option shows the dependence of the critical load on the radius r of the steel inclusion as shown in Fig. 2, while the concrete matrix size is kept fixed at a=150 mm. The paragraph above outlined that in the cases (A), (B), which behave similarly, there may appear a kink in the dependence of the critical load for some inclusion radius due to a change of stress magnitudes (of p_{n} and p_{t}) at the interface, while in the compression state of the case (C) no such a kink has appeared. Simultaneously, closeness of inclusion and outer matrix boundary also affect the results. Therefore, the stresses for the cases (A) and (C) are shown in Fig. 3 for a small inclusion and a large inclusion relatively to the matrix.

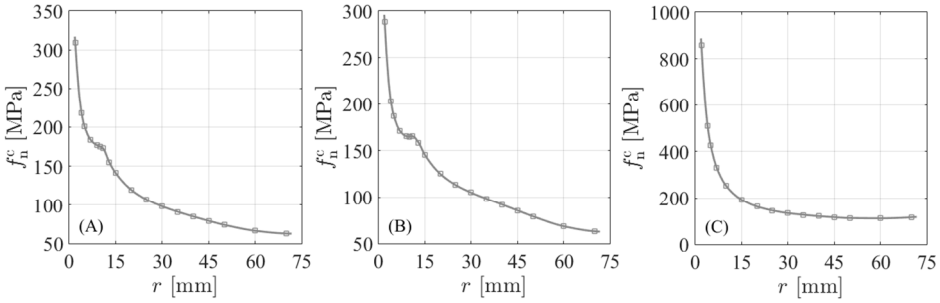

Fig. 2. Critical load for three types of boundary conditions: (A), (B), (C) according to Fig. 1, scaling of the inclusion with a=150 mm

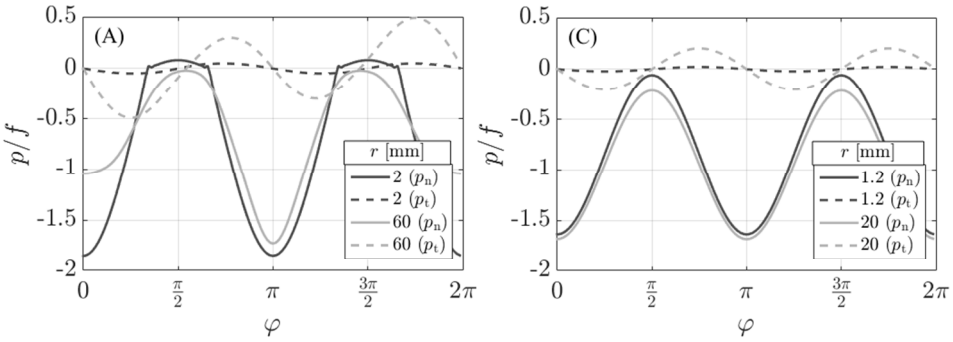

Fig. 3. Interface stresses for the constraints (A) and (C), a difference between small and big inclusions, scaled inclusion, a=150 mm

The graphs in the case (A) show different ratios between the stresses p_{n} and p_{t} so that a change in the character of the curve in Fig. 2 is easily explained: for small r maximal normal tensile stress is greater than the tangential one, therefore the crack develops in the opening mode, for big r the situation is opposite and

the appearing crack is rather in the shearing mode. This is also documented by Fig. 4 which shows the arising Mode I crack (clear opening) for a small fibre of radius r=2 mm and the form of Mode II crack for r=60 mm as it is also used in Fig. 3 for the case (A).

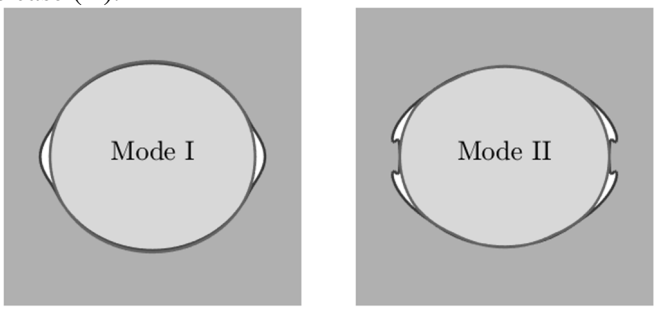

Fig. 4. Cracks at Mode I and Mode II

The effect of close contours is the most evident for the case (C) where the critical load $f_{\mathrm{n}}^{\mathrm{c}}$ has even increased a bit.

The second option for size changing mode shows the dependence of the critical load on the size a of the matrix as shown in Fig. 5. Here, the radius of the fibre is kept fixed r=10 mm. As before, in the cases (A), (B), there is a kink in the graph of the critical load for some matrix dimension caused by the observation demonstrated by Fig. 6 that, depending on the size of the matrix, either tensile normal or tangential stress is dominant at the instant of damage triggering. The graphs demonstrate various ratios between stresses p_{n} and p_{t} so that for the constraints (A) it causes different modes of the interface crack for various matrix sizes. This is the reason for the change of character of the curve in Fig. 5: for small a maximal tangential stress is greater than the tensile normal, therefore the tangential stress prevails to control the damage initiation, for big a the situation is opposite and the appearing crack is more in the opening mode. For the case (C), there is only compression.

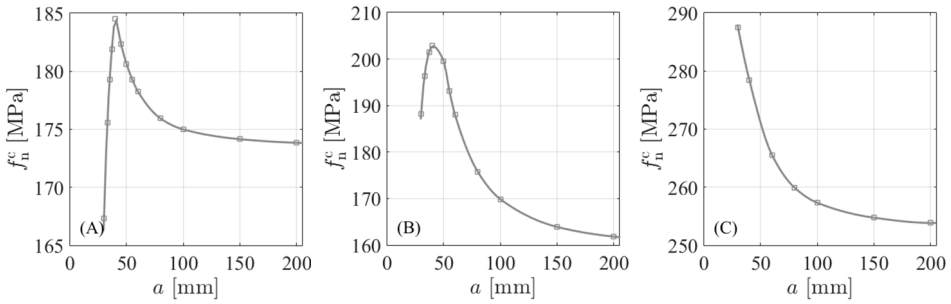

Fig. 5. Critical load for three types of boundary conditions: (A), (B), (C) according to Fig. 1, scaling of the matrix with r=10 mm

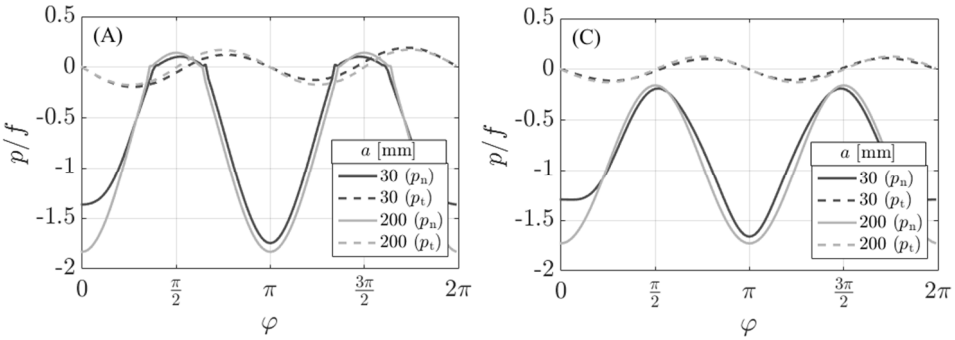

Fig. 6. Interface stresses for the constraints (A) and (C), a difference between small and large matrices, scaled matrix, r=10 mm

The last size changing mode provided the dependence of the critical load on the radius r of the inclusion as shown in Fig. 7. The ratio between structure's dimensions used in the test is $a{:}r$=75:4. Again, in the cases (A), (B), there is a kink of the graph in the middle of the shown span as, depending on the scale of the problem, either tensile normal or tangential stress is dominant at the instant of damage triggering, see also in Fig. 8. The figure shows the values of interface stresses relatively to the applied load f_n at the moment of damage initiation. The compressive forces, which are the greatest in fact, do not influence the damage process. The graphs reveal various ratios between maximal tensile normal and tangential stresses p_n and p_t, respectively. For the constraints (A) shown in Fig. 8, it causes different modes of the interface crack and it is the reason for the change of the slope of the curves in Fig. 7(A,B): for small r maximal normal tensile stress is greater than tangential, therefore the normal stress prevails to control the damage initiation, for big r the situation is opposite and the appearing crack is more in the shearing mode. For the constraints (C), again only tangential components affect damage triggering.

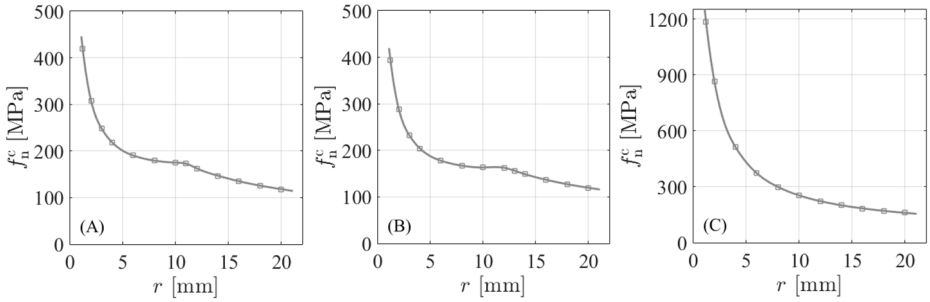

Fig. 7. Critical load for three types of boundary conditions: (A), (B), (C) according to Fig. 1, proportional scaling of the whole domain a/r=18.75

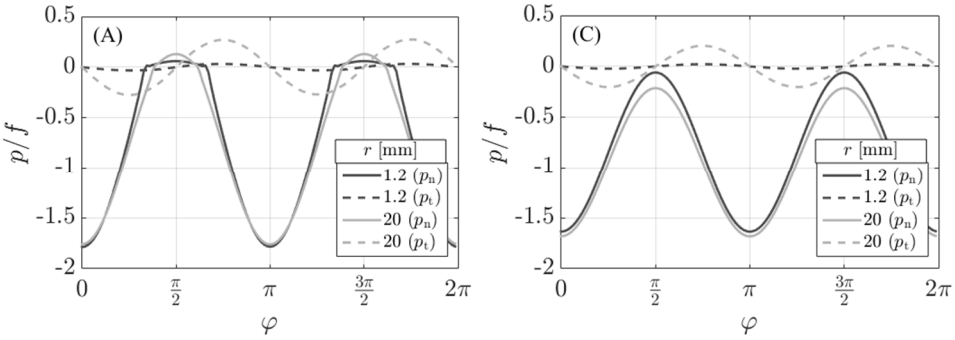

Fig. 8. Interface stresses for the constraints (A) and (C), a difference between small and big inclusions, proportional scaling, a/r=18.75

4. Conclusion

The influence of the steel reinforcement radius on crack initiation at the interface between the steel fibre and the concrete body of the structure was discussed using a numerical approach. The approach used a quasi-static delamination model for interface rupture based on an energetic approach with a cohesive zone interface. The obtained results confirm that the critical load which causes initiation of an interface crack strongly depends on sizes and ratios of the structural element dimensions. These geometric characteristics also affect the mode of the crack which appears at the interface. Nevertheless, this preliminary study provokes many questions about the interface properties or the applied load and their role in the discussed size effect: interfaces stiffnesses k, fracture energy G, used CZM model and its parameters, type of loading etc. A few such parametric studies will be analysed in the next future.

Acknowledgements: *The work was supported by the Ministry of Education, Science, Research and Sport of the Slovak Republic (Project VEGA 1/0078/16).*

References

[1] Carpinteri, A., Paggi, M., Zavarise, G. Snap-back instability in micro-structured composites and its connection with superplasticity, *Strength, Fracture and Complexity*, vol. 3, 2005, no. 2–4, p. 61–72.

[2] Cho, J., Joshi, M.S., Sun, C.T. Effect of inclusion size on mechanical properties of polymeric composites with micro and nano particles, *Composites Science and Technology*, vol. 66, 2006, no. 13, p. 1941–1952.

[3] Fisher, J.R., Gurland, J. Void nucleation in spheroidized carbon steels part 2: Model. *Metal science,* vol. 15, 1981, no 5, p. 193–202.

[4] Hutchinson, J.W., Suo Z. Mixed mode cracking in layered materials, *Advances in Applied Mechanics,* vol. 29, issue C, 1991, p. 63–191.

[5] Kšiňan, J., Vodička, R. A 2-D SGBEM formulation of contact models coupling the interface damage and Coulomb friction in fibre–matrix composites, *Engineering Fracture Mechanics*, vol. 168, 2016, p. 76–92.

[6] Mantič, V. Interface crack onset at a circular cylindrical inclusion under a remote transverse tension. Application of a coupled stress and energy criterion, *International Journal of Solids and Structures,* vol. 46, 2009, no 6, p. 1287–1304.

[7] Mantič, V., García, I.G. Crack onset and growth at the fibre-matrix interface under a remote biaxial transverse load. Application of a coupled stress and energy criterion, *International Journal of Solids and Structures*, vol. 49, 2012, no 17, p. 2273–2290.

[8] Roubíček T., Kružík M., Zeman J. Delamination and Adhesive Contact Models and their Mathematical Analysis and Numerical Treatment, In: *Mathematical Methods and Models in Composites* (Chapter 9), edited by V. Mantič, Imperial College Press, 2013, p. 349–400.

[9] Távara, L., Mantič, V., Graciani, E., París, F. BEM analysis of crack onset and propagation along fibre-matrix interface under transverse tension using a linear elastic-brittle interface model *Engineering Analysis with Boundary Elements,* vol. 35, 2011, no 2, p. 207–222.

[10] Vodička, R. A quasi-static interface damage model with cohesive cracks: SQP-SGBEM implementation, *Engineering Analysis with Boundary Elements,* vol. 62, 2016, p. 123–140.

[11] Vodička R., Mantič V. A multilinear cohesive law within a quasi-static interface damage model, *Discrete and Cont. Dynam. Syst.*, vol. 10, 2017, no. 6, p. 1539–1561.

[12] Vodička, R., Mantič, V., Roubíček, T. Energetic versus maximally-dissipative local solutions of a quasi-static rate-independent mixed-mode delamination model, *Meccanica*, vol. 49, 2014, no 12, p. 2933–2963.

Przesłano do redakcji: 24.03.2017 r.
Przyjęto do druku: 28.12.2018 r.